VERTICAL WATER VAPOR DISTRIBUTION AT PHOENIX

L. K. Tamppari, *Jet Propulsion Laboratory/Caltech, Pasadena, CA USA (leslie.tamppari@jpl.nasa.gov)*, **M. T. Lemmon,** *Department of Atmospheric Sciences, Texas A&M University, College Station, TX USA*.

Introduction:

The Phoenix and Mars Reconnaissance Orbiter (MRO) spacecraft participated together in an observation campaign that was a coordinated effort to study the Martian atmosphere. These coordinated observations were designed to provide near-simultaneous observations of the same column of atmosphere over the Phoenix lander. Seasonal coverage was obtained at L_s=5-10° resolution and diurnal coverage was obtained as often as possible and with as many times of day as possible. One key aspect of this observation set was the means to compare the amount of water measured in the whole column (via the MRO Compact Reconnaissance Imaging Spectrometer for Mars (CRISM; Murchie *et al*., 2007) and the Phoenix Surface Stereo Imager (SSI) with that measured at the surface (via the Phoenix Thermal and Electrical Conductivity probe (TECP; Zent *et al.*, 2008) which contained a humidity sensor). This comparison, along with the Phoenix LIDAR observations of the depth to which aerosols are mixed (Whiteway *et al.,* 2008, 2009), provides clues to the water vapor mixing ratio profile. Commonly, water vapor is assumed to be "well-mixed," in other words, a constant fraction of the atmospheric pressure for a given height (e.g., Smith et al., 2009; Smith, 2002). Typically, this assumption is made to an altitude at which clouds would condense given a related temperature profile.

Tamppari *et al.* (2009) showed that examination of a subset of these coordinated observations indicate that the water vapor is *not* well mixed in the atmosphere up to a cloud condensation height at the Phoenix location during northern summer, and results indicated that a large amount of water must be confined to the lowest 0.5-1 km. This is because if the near surface TECP humidity measured during daytime is taken as well mixed to a condensation height (about 8 km per TES seasonal T data) or even to the ~4 km top-of-boundary layer measured by LIDAR, then that exceeds the water column abundance measured by CRISM, indicating water cannot be well-mixed during the daytime at this season/location. Taking the TECP near-surface humidity measured at night and assuming well mixed, one derives far less water in the column than measured by CRISM or SSI, indicating that the near surface layer is depleted of water at night. Further, the total column abundance appears to change diurnally, both in CRISM data (may have been revised since Tamppari et al., 2009 publication) and SSI data (Fig. 1-1 and 1-2). These results lead to the conclusion that water exchanges with the surface on a diurnal basis.

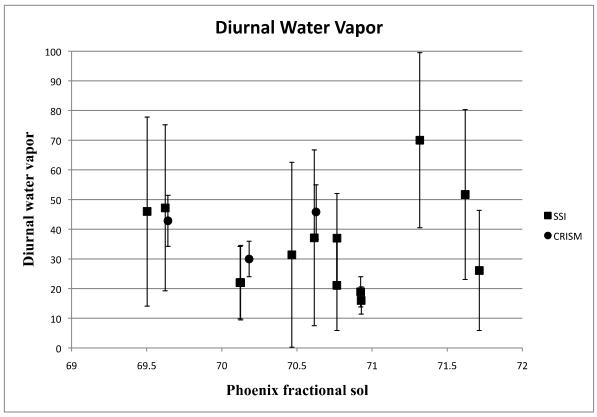

Figure 1-1. Diurnal water vapor measurements made by SSI (dots) and CRISM (squares) with error bars.

A key unknown is how deep the exchanging layer is, which is what we address with our modeling. Tamppari et al. (2009) showed that given a 15 pr μm diurnal change in column abundance combined with the TECP surface vapor pressure diurnal changes (~2.0 Pa to ≤0.1).

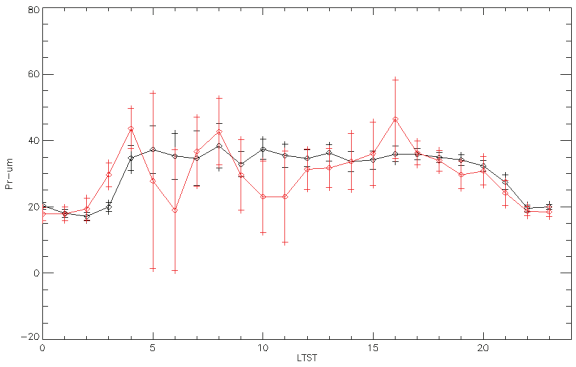

Figure 1-2. Diurnal change in water vapor column abundance as measured by SSI: averaged

over the Phoenix mission (black) and for Sols 60-80 (red).

Data Acquisition Strategy:

In order to detect water vapor using the Phoenix SSI camera, several water vapor filters were added [Lemmon et al., 2008]. They are: LA = 930.7 nm (broad), R4 = 935.5 nm (narrow), and R5 = 935.7 nm (narrow). The 935-nm filters are sensitive to water abundance above 5 pr microns in direct solar imaging. Because this band is weak, imaging of the horizon, opposite the sun is a more sensitive measure (Titov et al., 2000). Other continuum filters available in the SSI were used for comparison. For each observation set, we obtained images both above the sun and along the horizon opposite the sun. The above sun images are used for calibration, and the near-horizon images are used to detect water vapor. The approach to using the above-sun and horizon images is detailed in Titov et al. (2000). We have modified the strategy as described further below. We found that the Titov et al. approach of using the narrow neutral density filters was ineffective due to the low response even for long integration times. However, the broader LA filter was found to be sufficiently sensitive to water.

This water vapor data set was collected throughout the Phoenix mission. There were 13 coordinated observation datasets focused on water vapor taken over the course of the Phoenix mission, spanning L_s=83-140°. Not all opportunities afforded full diurnal coverage, due to spacecraft constraints. Some opportunities included only a few observations, but others afforded 6 throughout the diurnal cycle.

Data Analysis:

We have focused on a particular period of the Phoenix mission when we have a full complement of data sets and good diurnal coverage: Sol 70 (L_s ~108.3º). We have performed the majority of our testing on midday observations as they were more commonly taken during the mission.

We have evaluated our data using a Monte Carlo (MC) radiative transfer model to accurately capture the horizon geometry. It was found that this model did not provide a unique solution, given the natural uncertainty with a statistical model, even with a high number of trials. Because the model uncertainty was too large, we developed a hybrid DISORT-spherical model. (DISORT model, Stamnes et al. 1988), which uses DISORT for a diffuse light source function and accurate geometry for the camera line of sight. Within this framework, we have evaluated a variety of profile options to model: A 2-layer model (boundary layer and above boundary layer), a continuous model (no discontinuity in mixing ratio at the top of a boundary layer), and a gradient model (8 layers in boundary layer; 2 layers above, with selectable scale height in each layer).

Two-layer model. The two-layer model represents the boundary layer and the free atmosphere, with free parameters representing the water content of each and the height of the boundary. Exploring the water vapor profile space for our test case (Sol 70 midday), the best fits occur with a large amount of the total column of water (~30%) confined < 0.5 km. However, better fits will occur with the water confined very low, < 100 m. This code couples the dust and water profiles, but we know from LIDAR data that dust should be well mixed up to 4 km. Running vapor profiles that have water well mixed up to 4 km, and only varying the amount of water in that 4 km layer, cannot be modeled with any fidelity, so a large amount of water must be confined lower in the atmosphere. We have also performed sensitivity studies on the effects of different scale heights (controlling both water and dust). Results indicate the lower scale heights (from the nominal H=10.5 km) do not match the observations as well as the nominal H, but still show that a large percent of the total column abundance of water is confined within the bottom 1 km or less.

Given this best-fit of a 'water boundary layer' height (0.5 km) and total amount of water in that layer (10 pr microns), we used a water vapor profile model to determine the water vapor mixing ratios, applying the commensurate surface TECP data as a constraint, as well as the total water column abundance from CRISM and the likely cloud condensation height from MCS T profiles. We assume the water in the previously determined 'water boundary layer' is well mixed, then there (usually) is a discontinuity, and water above that 'water boundary layer' is well mixed at a different mixing ratio up to a cloud condensation height and then follows the cloud condensation curve above that. The best match results show that the mass mixing ratio at the surface is about 1115 ppmm for the bottom 0.5 km and then 130 ppmm above that to a cloud condensation level, and then the water vapor amount follows a cloud condensation curve.

Our uncertainty metric for this two-layer model is higher than desired. In order to examine the sensitivity of the quality of the fit to uncertainties in other parameters, we varied the total column abundance of water. The uncertainty in the CRISM data is 10% (Smith et al., 2009), so we examined a case with 10% lower total column water and the uncertainty in the fit came down to an acceptable level. The solution gave the same 'water boundary layer' of 0.5 km indicating 1115 ppmm in that layer, but since the total column was reduced, our vapor profile model shows a reduction to 115 ppmm in the layer above.

Because a sharp discontinuity between a layer with a high water mixing ratio and one with a lower

vapor mixing ratio seems unlikely, we examined other models as described below.

Continuous model. The continuous model forced there to be no discontinuity in water concentration; it included a fixed concentration above the boundary layer and a gradient within the boundary layer. The relative abundances of water in the two layers was calculated from the resulting profile. No parameter values resulted in adequate fits to the data.

Gradient model. The gradient model is a generalization of the previous two, with a gradient in the boundary layer, a fixed concentration above the layer, and an allowed discontinuity at the boundary. The altitude was fixed at 4 km based on LIDAR results [Whiteway et al., 2009]. Results from this model will be presented.

Conclusions and Future Work:

Our current analysis indicates that there is a large percentage of the column water vapor abundance confined near the subsurface. Improvements to the model have been made and recent analysis using this model and comparing to earlier results will be presented. In the future, we will evaluate other midday cases and compare to the Sol 70 case. Then we will evaluate data taken at other times of day (morning, evening, "night") and expand our analysis to include data taken over the course of the Phoenix mission.

References:

Murchie, S. *et al.* (2007). *J. Geophys. Res*., 112 (E05S03), doi:10.1029/2006JE002682.

Whiteway, J. M. *et al.* (2008). Lidar on the Phoenix mission to Mars, *J. Geophys. Res.*, 113, E00A08, doi:10.1029/2007JE003002.

Whiteway, J. M. *et al.* (2009). Mars water-ice clouds and precipitation, *Science* 325 (5936), p. 68.

Smith, M. D. (2002). *J. Geophys. Res.* 107 (E11), p. 5115, doi:10.1029/2001JE001522.

Smith, M. D. *et al.* (2009). J. *Geophys. Res.*, 114, E00D03, doi:10.1029/2008JE003288.

Tamppari, L. K. *et al.* **(**2009). *J. Geophys. Res.*, 115, E00E17, doi:10.1029/2009JE003415, 2010

Titov, D. V. *et al.* (2000). *Plan. and Sp. Sci.,* 48, pp. 1423-1427.

Lemmon, M.T. *et al.* (2008). *Lunar and Planetary Institute Science Conference Abstracts* 39, 2156.

Stamnes, K. *et al.* (1988). *Appl. Opt*. 27, 2502.